Molecular Cell
Short Article

A Selective Requirement for 53BP1 in the Biological Response to Genomic Instability Induced by Brca1 Deficiency

Liu Cao,[1,2,*] Xioaling Xu,[2,6] Samuel F. Bunting,[3,6] Jie Liu,[1] Rui-Hong Wang,[2] Longyue L. Cao,[1,2] J. Julie Wu,[1] Tie-Nan Peng,[4] Junjie Chen,[5] Andre Nussenzweig,[3] Chu-Xia Deng,[2,*] and Toren Finkel[1,*]
[1]Translational Medicine Branch, National Heart, Lung and Blood Institute
[2]Genetics of Development and Disease Branch, National Institute of Diabetes and Digestive and Kidney Diseases
[3]Experimental Immunology Branch, National Cancer Institute
National Institutes of Health, Bethesda, MD 20892, USA
[4]Department of Oral and Maxillofacial Surgery, Stomatological College, JiLin University, Changchun City, Jilin Province 130041, China
[5]Department of Therapeutic Radiology, Yale University School of Medicine, New Haven, CT 06520, USA
[6]These authors contributed equally to this work
*Correspondence: liu.cao@nih.gov (L.C.), chuxiad@bdg10.niddk.nih.gov (C.-X.D.), finkelt@nih.gov (T.F.)
DOI 10.1016/j.molcel.2009.06.037

SUMMARY

The molecular pathways leading from genomic instability to cellular senescence and/or cell death remain incompletely characterized. Using mouse embryonic fibroblasts with constitutively increased DNA damage due to the absence of the full-length form of the tumor suppressor Brca1 (*Brca1*$^{\Delta11/\Delta11}$), we show that deletion of p53 binding protein 1 (53BP1) selectivity abrogates senescence and cell death stimulated by reduced Brca1 activity. Furthermore, the embryonic lethality induced by Brca1 mutation can be alleviated by 53BP1 deletion. Adult *Brca1*$^{\Delta11/\Delta11}$*53BP1*$^{-/-}$ manifest constitutively high levels of genomic instability, yet age relatively normally, with a surprisingly low incidence of overall tumor formation. Together, these in vitro and in vivo data suggest that 53BP1 is specifically required for the development of premature senescence and apoptosis induced by Brca1 deficiency. These observations may have important implications for Brca1-mediated tumor formation as well as for the molecular pathway leading from genomic instability to organismal aging.

INTRODUCTION

DNA damage induces a range of cellular responses from growth arrest to the induction of senescence or apoptosis. It is generally believed that in the setting of such damage, the lack of cellular proliferation or the loss of cell viability provides an efficient tumor suppressor mechanism. While inhibiting cancer, the accumulation of senescent and apoptotic cells can also contribute to and potentially augment the rate of organismal aging. Indeed, a number of mammalian models of chronic DNA damage and genomic instability are characterized by exhibiting both a tumor-prone and accelerated aging phenotype (Chen et al., 2007; Lombard et al., 2005; Serrano and Blasco, 2007).

Brca1 is an important checkpoint and DNA damage repair gene that is required for maintaining genomic integrity. We have previously described a mouse model of constitutive DNA damage in which exon 11 of the *Brca1* gene has been deleted, resulting in the absence of the full-length *Brca1* isoform. Similar to *Brca1* null mice, the *Brca1*$^{\Delta11/\Delta11}$ mice in general die in utero, although this embryonic lethality happens slightly later in development in the *Brca1*$^{\Delta11/\Delta11}$ animals than in the null embryos (Hakem et al., 1997; Ludwig et al., 1997; Xu et al., 2001). Further analysis of *Brca1*$^{\Delta11/\Delta11}$ embryos has demonstrated that there is a significant increase in both spontaneous cell death and cellular senescence (Cao et al., 2003, 2006; Xu et al., 2001). Although the observed embryonic lethality of *Brca1*$^{\Delta11/\Delta11}$ mice can be rescued by deletion of one allele of *p53*, the resulting *Brca1*$^{\Delta11/\Delta11}$*p53*$^{+/-}$ mice exhibit a high rate of spontaneous tumor formation in multiple organs (Xu et al., 2001). Detailed molecular analysis of these malignancies has demonstrated that essentially all of the tumors that arise are accompanied by a loss of heterozygosity in the *p53* locus (Brodie et al., 2001; Cao et al., 2006). In addition to this tumor-prone phenotype, the *Brca1*$^{\Delta11/\Delta11}$*p53*$^{+/-}$ mice also exhibit many features that are consistent with accelerated aging (Cao et al., 2003, 2006).

The embryonic lethality of the *Brca1*$^{\Delta11/\Delta11}$ mice can also be rescued by deletion of certain components of the DNA damage pathway (DDR), including ATM and Chk2 (Cao et al., 2006). Here, we have further characterized the in vitro and in vivo pathways activated in *Brca1*$^{\Delta11/\Delta11}$ mice. Our results identify 53BP1 as essential for mediating cell death and senescence induced by *Brca1* deficiency, but dispensable for apoptosis and senescence induced by a variety of other DNA damaging agents.

RESULTS

Mouse embryonic fibroblasts (MEFs) isolated from *Brca1*$^{\Delta11/\Delta11}$ mice are known to undergo rapid premature senescence in culture, since these cells manifest a constitutive increase in

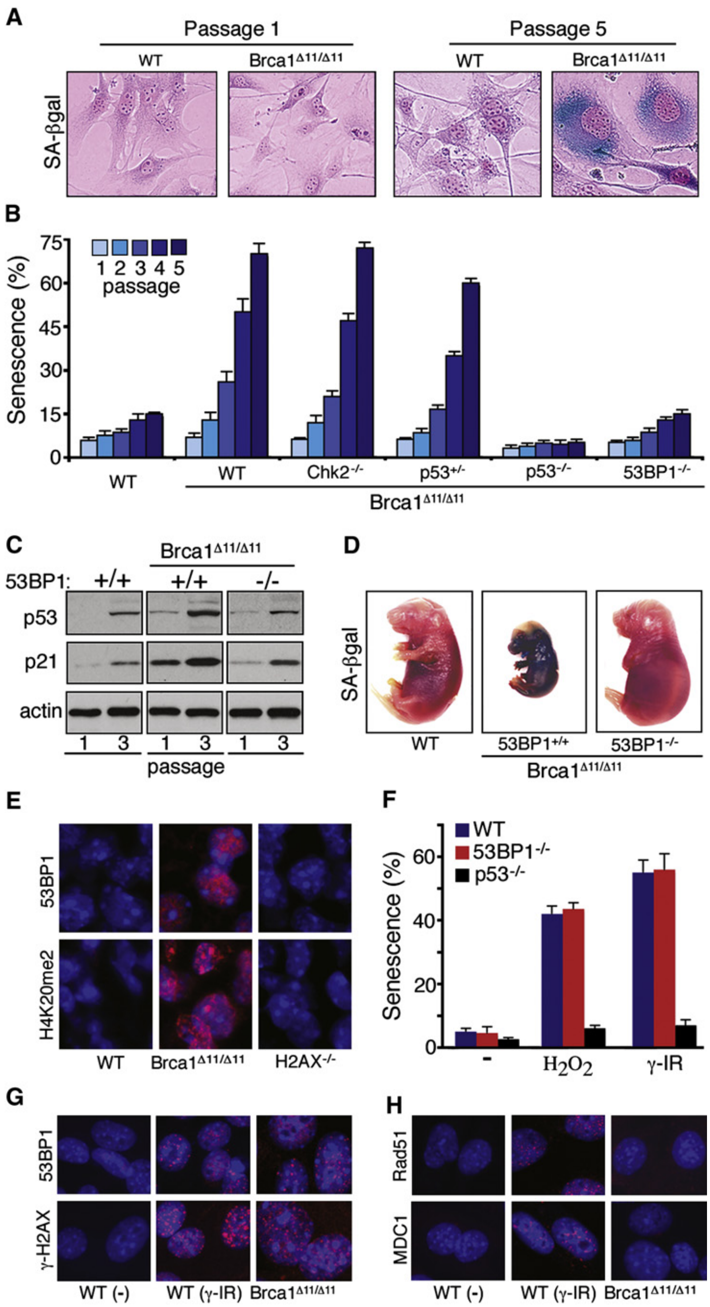

Figure 1. Deletion of *53BP1* Selectively Rescues Premature Senescence Due to Reduced Brca1 Activity

(A) MEFs derived from *Brca1*$^{\Delta11/\Delta11}$ embryos rapidly develop morphological evidence for premature senescence, including positive SA-βgal staining.

(B) Quantification of SA-βgal staining in MEFs derived from the indicated genotypes (mean ± SD).

(C) Levels of p53 protein and its transcriptional target p21 in early-passage MEFs. The deletion of *53BP1* appears to inhibit the observed activation of p53 in *Brca1*$^{\Delta11/\Delta11}$ MEFs.

(D) SA-βgal staining of E18 embryos.

(E) Sections of brain obtained from WT, *Brca1*$^{\Delta11/\Delta11}$, or *H2AX*$^{-/-}$ embryos were assessed for nuclear foci of 53BP1 or level of histone H4-dimethylated lysine 20 (H4K20me2). Nuclei were visualized by DAPI (blue) staining.

(F) Observed senescence following exposure to hydrogen peroxide (20 μM) or γ irradiation (γ-IR) (10 Gy) in WT MEFs or MEFs lacking *53BP1* or *p53* (mean ± SD).

(G) Characterization of 53BP1 and γ-H2AX foci in WT or *Brca1*$^{\Delta11/\Delta11}$ MEFs. Where indicated, WT MEFs were analyzed 3 hr after 10 Gy irradiation (γ irradiation).

(H) Similar conditions were used to assess for the presence of nuclear foci containing Rad51 and MDC1.

DNA damage secondary to reduced Brca1 activity (Cao et al., 2003, 2006). Using these MEFs, along with a candidate gene approach, we sought to identify genes specifically required for Brca1-mediated premature senescence. In culture, *Brca1*$^{\Delta11/\Delta11}$ MEFs rapidly manifest a senescent morphology (Figure 1A) and exhibit positive staining for senescence-associated β-galactosidase (SA-βgal). By passage 5, nearly 75% of MEFs isolated from *Brca1*$^{\Delta11/\Delta11}$ mice were SA-βgal positive (Figure 1B).

Based on our previous observations (Cao et al., 2003, 2006; Xu et al., 2001), we asked whether perturbation of various DDR or cell cycle-regulatory components could rescue *Brca1*$^{\Delta11/\Delta11}$-mediated premature senescence. MEFs were prepared from crosses between *Brca1*$^{+/\Delta11}$ mice and various other animals containing targeted deletions of genes within these identified pathways. As noted in Figure 1B, although *Chk2* deletion can rescue the *Brca1*$^{\Delta11/\Delta11}$ embryonic lethality (Cao et al., 2006), *Brca1*$^{\Delta11/\Delta11}$ *Chk2*$^{-/-}$ MEFs appear to prematurely senesce at the same elevated rate as *Brca1*$^{\Delta11/\Delta11}$ cells. In contrast, deletion of one allele of *p53* resulted in a small reduction in the rate of *Brca1*$^{\Delta11/\Delta11}$-induced senescence, while deletion of both *p53* alleles appeared to completely abrogate the observed *Brca1*$^{\Delta11/\Delta11}$-stimulated premature senescence. Such results were not unexpected, as *p53* deletion abrogates senescence induced by numerous stimuli (Riley et al., 2008; Rodier et al., 2007). Similar analysis with MEFs containing targeted deletions of *ATM*, *Chk1*, *H2AX*, *p21*, *PTEN*, *Gadd45a*, *p19*^{ARF}, and *Parp1* revealed that none of these gene deletions could rescue premature senescence caused by reduced Brca1 activity (unpublished data). In contrast, we observed that *Brca1*$^{\Delta11/\Delta11}$ MEFs lacking 53BP1, a DNA damage-response and p53-binding protein (Adams and Carpenter, 2006), were seemingly resistant to the observed accelerated senescence (Figure 1B). Similarly, while *Brca1*$^{\Delta11/\Delta11}$ MEFs appeared to have increased levels of p53 and evidence for increased p53 activity (Figure 1C), these biochemical changes were not evident in *Brca1*$^{\Delta11/\Delta11}$*53BP1*$^{-/-}$ MEFs.

To assess whether 53BP1 could also rescue *Brca1*$^{\Delta11/\Delta11}$-mediated senescence in vivo, we took advantage of previous observations that developing *Brca1*$^{\Delta11/\Delta11}$ embryos manifest an intense senescence-mediated growth arrest (Cao et al., 2003, 2006). Consistent with those previous reports, *Brca*1$^{\Delta11/\Delta11}$ embryos were smaller than wild-type embryos and stained intensely positive for SA-βgal (Figure 1D). This premature embryonic senescence was noticeably absent in *Brca1*$^{\Delta11/\Delta11}$*53BP1*$^{-/-}$

embryos. Interestingly, *Brca1*$^{\Delta11/\Delta11}$ embryos exhibited evidence for constitutive 53BP1 activation (Figure 1E). This response appeared relatively specific, as a similar activation was not evident in *H2AX*$^{-/-}$ embryos, even though H2AX is also required for the maintenance of genomic stability (Celeste et al., 2002). Previous results have documented that 53BP1 recruitment to DNA requires specific alterations in histone lysine methylation (Botuyan et al., 2006; Huyen et al., 2004). Consistent with these observations, we observed increased staining for histone H4-dimethylated lysine 20 in *Brca1*$^{\Delta11/\Delta11}$ embryos, but not in *H2AX*$^{-/-}$ embryos (Figure 1E). Other histone modifications known to act as lower-affinity binding sites for 53BP1 were also selectively observed in *Brca1*$^{\Delta11/\Delta11}$ embryos (Figure S1).

Given that *53BP1* deletion rescued senescence induced by reduced Brca1 activity, we next asked what role 53BP1 played in other pathways leading to cellular senescence. The growth of MEFs in 20% oxygen results in passage-dependent accumulation of senescent cells that in rodent fibroblasts appears to be a stress-mediated, "culture shock"-like phenomenon (Parrinello et al., 2003). As expected, WT MEFs had a passage-dependent increase in senescence and a corresponding increase in p53 levels and activity under these growth conditions (Figure S2). An identical biological and biochemical response was seen in *53BP1*$^{-/-}$ MEFs. In contrast, *p53*$^{-/-}$ MEFs had a complete abrogation of this senescent response (Figure S2). A similar analysis employing other triggers of senescence, including oxidative stress with exogenous hydrogen peroxide or γ irradiation, demonstrated that WT and *53BP1*$^{-/-}$ MEFs responded similarly (Figure 1F). In contrast, in *p53*$^{-/-}$ MEFs, the induction of senescence following these stresses was severely compromised or absent.

The above observations suggest that 53BP1 plays a specific role in *Brca1*$^{\Delta11/\Delta11}$-mediated senescence. To begin to try and understand the basis of the specificity, we sought to analyze and compare the cellular response to reduced Brca1 activity to the response observed with other forms of DNA damage. In MEFs, both irradiation and Brca1 deficiency resulted in activation of 53BP1 and H2AX (Figure 1G). As previously described, in both irradiated cells and in cells treated with hydrogen peroxide (Figure S3), these DNA damage foci also appeared to recruit additional factors, including RAD51 and MDC1 (van Attikum and Gasser, 2009). Interestingly, the recruitment of both RAD51 and MDC1 was not evident in *Brca1*$^{\Delta11/\Delta11}$ MEFs (Figure 1H). This suggests that the DNA damage foci formed in the setting of reduced Brca1 activity are qualitatively different than what is observed with other DNA-damaging stresses.

In addition to inducing cellular senescence, the *Brca1*$^{\Delta11/\Delta11}$ mutation can also trigger programmed cell death, and this is particularly evident within the developing embryo (Cao et al., 2003, 2006; Xu et al., 2001). We therefore analyzed rates of apoptosis in WT, *Brca1*$^{\Delta11/\Delta11}$, or *Brca1*$^{\Delta11/\Delta11}$*53BP1*$^{-/-}$ embryos. Similar to our observations regarding *Brca1*$^{\Delta11/\Delta11}$-mediated senescence, deletion of *53BP1* appeared to dramatically rescue *Brca1*$^{\Delta11/\Delta11}$-mediated cell death (Figures 2A and 2B).

The ability of *53BP1* deletion to rescue in vivo embryonic senescence and apoptosis stimulated by the lack of Brca1 activity suggested that *53BP1* deletion might rescue the overall embryonic lethality caused by decreased Brca1 activity (Cao et al., 2003, 2006; Xu et al., 2001). Indeed, numerous healthy offspring were obtained in the setting of *Brca1*$^{\Delta11/\Delta11}$ along with deletion of *53BP1*, while we observed no viable offspring of *Brca1*$^{\Delta11/\Delta11}$ mice containing both copies of *53BP1* and only very rare survival of *Brca1*$^{\Delta11/\Delta11}$*53BP1*$^{+/-}$ mice (Table 1). Again, *53BP1* appeared unique in this role, as we observed no viable *Brca1*$^{\Delta11/\Delta11}$*H2AX*$^{-/-}$ mice (Table S1).

The survival of *Brca1*$^{\Delta11/\Delta11}$*53BP1*$^{-/-}$ mice allowed us to assess whether cells from these animals manifested a generalized alteration in their apoptotic threshold. As expected, γ irradiation triggered a significant increase in apoptosis of WT thymocytes (Figure 2C). This response was unaltered in *53BP1*$^{-/-}$ thymocytes, both in terms of the degree of cell death as well as the DDR signaling pathway triggered by irradiation (Figure 2D). Similarly, thymocytes obtained from *Brca1*$^{\Delta11/\Delta11}$ *53BP1*$^{-/-}$ mice had similar biological and biochemical responses to irradiation when compared to WT cells (Figures 2C and 2D). In contrast, numerous previous studies have demonstrated that thymocytes obtained from either *p53*$^{-/-}$ or *Chk2*$^{-/-}$ mice are significantly impaired in their ability to undergo apoptosis following irradiation (Clarke et al., 1993; Hirao et al., 2000; Lowe et al., 1993). A similar analysis in MEFs demonstrated that *53BP1*$^{-/-}$ cells had intact and, in some cases, even an augmented apoptotic response following exposure to hydrogen peroxide, doxorubicin, or γ irradiation (Figure 2E).

One potential explanation for the ability of *53BP1* deletion to rescue mice expressing *Brca1*$^{\Delta11/\Delta11}$ is that 53BP1 somehow altered or reduced the level of DNA damage and genomic instability in *Brca1*$^{\Delta11/\Delta11}$-expressing cells and tissues. To exclude this possibility, we analyzed the activation of the DDR in *Brca1*$^{\Delta11/\Delta11}$ or *Brca1*$^{\Delta11/\Delta11}$*53BP1*$^{-/-}$ cells, making use of our previous observation that nuclear foci of γ-H2AX were evident in *Brca1*$^{\Delta11/\Delta11}$ MEFs (Figure 1G). Overall, the degree of H2AX nuclear foci appeared similar when comparing MEFs (Figures 3A and 3B) or embryonic tissues (Figures 3C–3E) derived from either *Brca1*$^{\Delta11/\Delta11}$ or *Brca1*$^{\Delta11/\Delta11}$*53BP1*$^{-/-}$ mice. Similarly, metaphase spreads derived from *Brca1*$^{\Delta11/\Delta11}$*53BP1*$^{-/-}$ adult B cells exhibited genomic instability (Figures 3F and 3G).

We next sought to analyze the overall biological consequences of *53BP1* deletion in the setting of the *Brca1*$^{\Delta11/\Delta11}$ expression. After weaning, *Brca1*$^{\Delta11/\Delta11}$*53BP1*$^{-/-}$ as well as *53BP1*$^{-/-}$ mice appeared outwardly healthy (Figure 4A), although by 3 months of age, mice deficient in *53BP1* exhibited a very modest but significant weight reduction compared to WT mice (Figure S4). Similarly, at a year of age, *Brca1*$^{\Delta11/\Delta11}$ *53BP1*$^{-/-}$ mice continued to weigh and to appear essentially indistinguishable from WT mice (Figure S5). In contrast, *Brca1*$^{\Delta11/\Delta11}$ animals rescued by haploinsufficiency of *p53* weighed only 70% as much as WT mice at 1 month of age and approximately 50% of WT animals at 7 months of age (Cao et al., 2003, 2006).

In contrast to *Brca1*$^{\Delta11/\Delta11}$*53BP1*$^{-/-}$ mice, by 7 months of age, *Brca1*$^{\Delta11/\Delta11}$*p53*$^{+/-}$ mice exhibited clear evidence of accelerated aging (Figure 4A). This included, among other signs, the development of marked kyphosis, as well as changes in the animal's coat and overall physical activity. We also observed increased senescence in *Brca1*$^{\Delta11/\Delta11}$*p53*$^{+/-}$ tissues when compared to

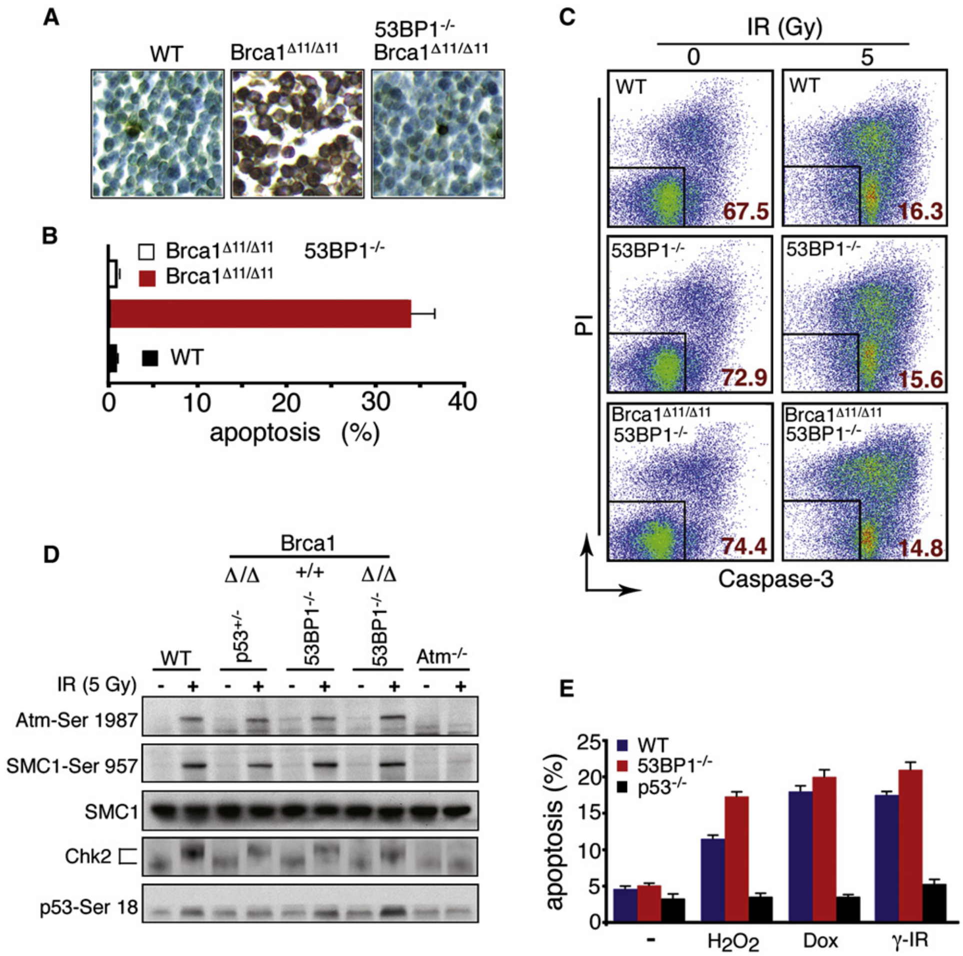

Figure 2. Deletion of *53BP1* Selectively Rescues *Brca1*$^{\Delta11/\Delta11}$-Mediated Cell Death

(A) Representative TUNEL staining observed in the brain of E18 embryos.

(B) Quantification of apoptosis in WT, *Brca1*$^{\Delta11/\Delta11}$, or *Brca1*$^{\Delta11/\Delta11}$*53BP1*$^{-/-}$ embryos (mean ± SD).

(C) Radiation-induced cell death observed in WT, *53BP1*$^{-/-}$, and *Brca1*$^{\Delta11/\Delta11}$*53BP1*$^{-/-}$ thymocytes was similar. The box in the lower left hand represents non-apoptotic thymocytes, and the percentage of such cells is displayed in the lower right-hand corner.

(D) Analysis of the DDR in basal and irradiated thymocytes bearing the indicated genotype.

(E) Cell death (mean ± SD) in WT, *53BP1*$^{-/-}$, or *p53*$^{-/-}$ MEFs following exposure to hydrogen peroxide (50 μM), doxorubicin (200 ng/ml), and γ irradiation (15 Gy).

WT or *Brca1*$^{\Delta11/\Delta11}$*53BP1*$^{-/-}$ tissues (Figure 4B). Similarly, assessment of the rates of spontaneous apoptosis in rapidly dividing organs such as the intestine revealed that *Brca1*$^{\Delta11/\Delta11}$ expression triggered significantly increased cell death in *p53*$^{+/-}$-rescued mice, but not in *Brca1*$^{\Delta11/\Delta11}$*53BP1*$^{-/-}$ mice (Figure 4C). Consistent with this increase in cell death, *Brca1*$^{\Delta11/\Delta11}$*p53*$^{+/-}$ cells had a constitutive activation of p53 not observed in cells obtained from either *53BP1*$^{-/-}$ or *Brca1*$^{\Delta11/\Delta11}$*53BP1*$^{-/-}$ mice (Figure S6).

Given that accumulation of senescent cells and increased cell death are both thought to mediate the accelerated aging phenotypes seen in models of chronic DNA damage, we next sought to assess the rate of aging in *Brca1*$^{\Delta11/\Delta11}$ mice that were rescued by either *53BP1* deletion or by haploinsufficiency of *p53*. As

Table 1. Predicted and Observed Offspring of Brca1 Mutant Mice with the Indicated 53BP1 Status

Crosses	*Brca1*$^{+/\Delta11}$*53BP1*$^{+/-}$ x *Brca1*$^{+/\Delta11}$*53BP1*$^{+/-}$			*Brca1*$^{+/\Delta11}$*53BP1*$^{-/-}$ x *Brca1*$^{+/\Delta11}$*53BP1*$^{-/-}$		
Total offspring	148			251		
Genotypes	*Brca1*$^{\Delta11/\Delta11}$ *53BP1*$^{+/+}$	*Brca1*$^{\Delta11/\Delta11}$ *53BP1*$^{+/-}$	*Brca1*$^{\Delta11/\Delta11}$ *53BP1*$^{-/-}$	*Brca1*$^{+/+}$ *53BP1*$^{-/-}$	*Brca1*$^{+/\Delta11}$ *53BP1*$^{-/-}$	*Brca1*$^{\Delta11/\Delta11}$ *53BP1*$^{-/-}$
Predicted number	9.25	20	9.25	62.8	125.5	62.8
Observed number	0	1	8	65	130	56

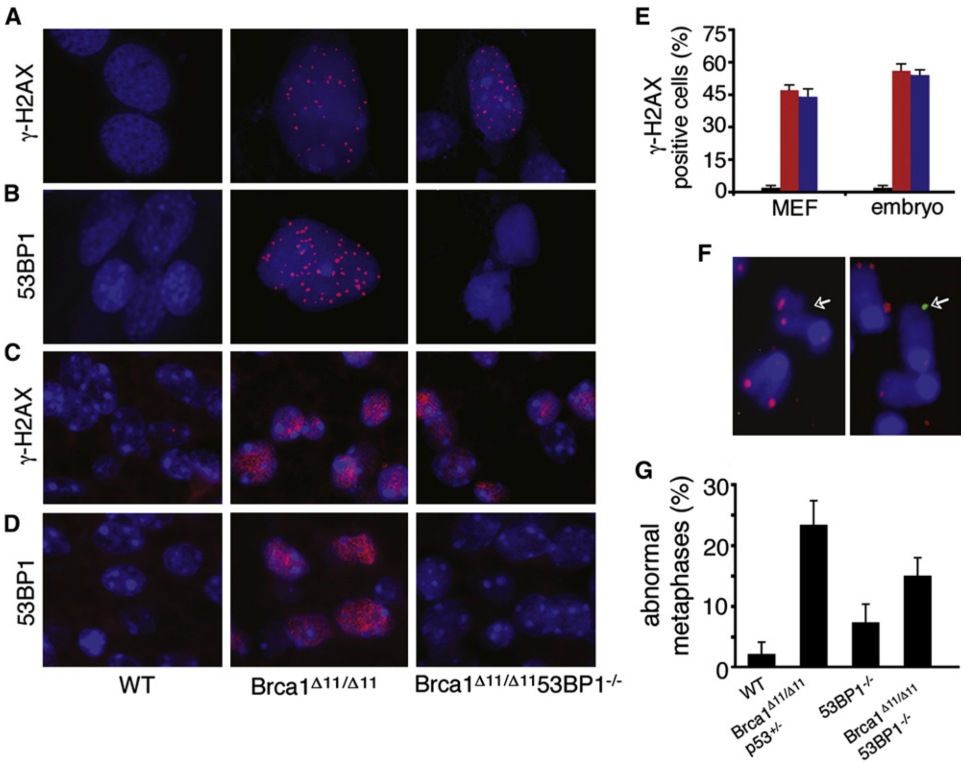

Figure 3. Deletion of *53BP1* Does Not Alter *Brca1*$^{\Delta11/\Delta11}$-Mediated Genomic Instability

(A and B) Early-passage MEFs were assessed for evidence of activation of the DDR, including nuclear foci of γ-H2AX (A) and 53BP1 (B).

(C and D) Day E16 brains were analyzed for nuclear foci of γ-H2AX (C) or 53BP1 (D), demonstrating the activation of the DDR in all *Brca1*$^{\Delta11/\Delta11}$-expressing embryos.

(E) Quantification of γ-H2AX activation in WT (black), *Brca1*$^{\Delta11/\Delta11}$ (red), or *Brca1*$^{\Delta11/\Delta11}$*53BP1*$^{-/-}$ (blue) MEFs and embryos (mean ± SD).

(F) Metaphase spreads from B cells obtained from *Brca1*$^{\Delta11/\Delta11}$*53BP1*$^{-/-}$ mice. Arrow in left panel denotes the presence of a chromatid break. Right panel demonstrates a chromosomal 12 break at the IgH locus. Chromosomes were stained with probes for the IgH locus (green) and a telomere-specific probe (red) and counterstained with DAPI (blue).

(G) Percentage of abnormal metaphase spreads (mean ± SD) obtained from adult B cells with the indicated genotype (n = 3 animals per genotype with at least 50 metaphase spreads per animal).

noted above, the latter mice exhibited increased tissue senescence and apoptosis triggered by *Brca1*$^{\Delta11/\Delta11}$ expression, while in *53BP1*$^{-/-}$-rescued mice, these responses were largely absent. Analysis of skin thickness (Figure 4D) and bone density (Figure S7) revealed that the changes associated with accelerated aging present in *Brca1*$^{\Delta11/\Delta11}$*p53*$^{+/-}$ mice were not evident in *Brca1*$^{\Delta11/\Delta11}$*53BP1*$^{-/-}$ animals. This point is reinforced by the analysis of overall life span. As opposed to *Brca1*$^{\Delta11/\Delta11}$*p53*$^{+/-}$ mice, whose maximal life span is roughly 1 year, nearly 80% of *Brca1*$^{\Delta11/\Delta11}$*53BP1*$^{-/-}$ were still alive at 20 months (Figure 4E).

Finally, we have previously reported that *Brca1*$^{\Delta11/\Delta11}$ mice rescued by homozygous deletion of *p53* rapidly develop multiple tumors (Brodie et al., 2001; Cao et al., 2006; Xu et al., 2001). We observed a similar high rate of cancer deaths in *Brca1*$^{\Delta11/\Delta11}$ *p53*$^{+/-}$ mice, with a median tumor-free survival time of approximately 9 months (Figure 4F). In contrast, and somewhat unexpectedly, *Brca1*$^{\Delta11/\Delta11}$ mice lacking *53BP1* exhibited only a very modest rate of cancer formation (<10%) in the first 20 months of life. Analysis of the tumors that developed in these animals demonstrated an absence of breast cancer; rather, the tumor spectrum closely mirrored what has been previously observed in *53BP1*-deficient mice, with all tumors in the first 18 months consisting of thymic lymphomas (Ward et al., 2003).

DISCUSSION

In summary, we have demonstrated that 53BP1 is required for the induction of senescence or apoptosis triggered by reduced Brca1 activity. Interestingly, although *53BP1* deletion abrogates these responses in the setting of reduced Brca1 activity, the absence of 53BP1 does not appear to modulate the induction of senescence or apoptosis triggered by other stimuli. This selectivity stands in contrast to other genetic manipulations, such as deletion of *p53*, that block senescence and apoptosis mediated not only by Brca1, but for a wide range of DNA-damaging stresses. Although the precise mechanism underlying this selectivity is unknown, the overall composition of DNA-damage foci formed in *Brca1*-deficient cells is significantly different from those foci formed in the setting of exogenous DNA damage. Both irradiation and oxidative stress recruit a number of proteins, such as Rad51 and MDC1, that are not seen in the foci formed in *Brca1*$^{\Delta11/\Delta11}$ cells. We speculate that in the setting of these

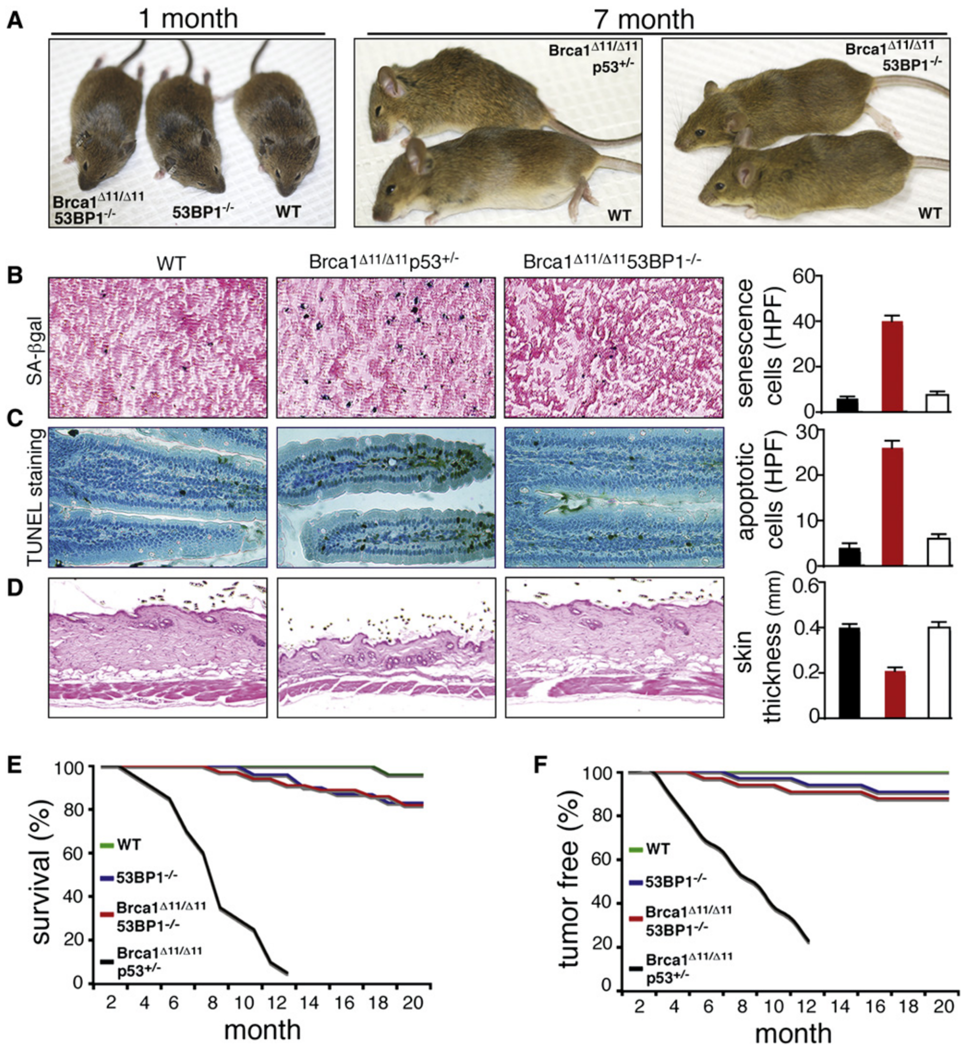

Figure 4. Deletion of *53BP1* Rescues the Premature Aging Phenotype Observed in *Brca1*$^{\Delta11/\Delta11}$ Mice without Significantly Increasing the Rates of Tumorgenesis

(A) Appearance of mice at 1 month of age, demonstrating that *Brca1*$^{\Delta11/\Delta11}$*53BP1*$^{-/-}$ animals appear virtually indistinguishable from WT mice (left panel). By 7 months, *Brca1*$^{\Delta11/\Delta11}$*p53*$^{+/-}$ mice develop changes associated with accelerated aging (middle panel), while *Brca1*$^{\Delta11/\Delta11}$*53BP1*$^{-/-}$ continue to appear similar to WT animals (right panel).

(B) Representative SA-βgal staining in the brain of 7-month-old animals, demonstrating increased tissue senescence in the *Brca1*$^{\Delta11/\Delta11}$*p53*$^{+/-}$ animals. Quantification (mean ± SD) of senescent cells per random high power field (HPF) is shown for WT (black bar), *Brca1*$^{\Delta11/\Delta11}$*p53*$^{+/-}$ (red bar), and *Brca1*$^{\Delta11/\Delta11}$*53BP1*$^{-/-}$ animals (open bar).

(C) Representative TUNEL staining in the intestine of 7-month-old mice.

(D) Sections of skin at 7 months, demonstrating age-related changes in the *Brca1*$^{\Delta11/\Delta11}$*p53*$^{+/-}$ mice, including reduced skin thickness and loss of subcutaneous adiposity.

(E) Overall survival of mice with the indicated genotypes, demonstrating that in comparison to *Brca1*$^{\Delta11/\Delta11}$ mice rescued by deletion of one allele of *p53*, *53BP1* deletion extends life span.

(F) Rates of tumor-free survival, demonstrating that a high percentage of *Brca1*$^{\Delta11/\Delta11}$*p53*$^{+/-}$ mice develop cancer, while this is largely absent in the *Brca1*$^{\Delta11/\Delta11}$ *53BP1*$^{-/-}$ animals. The number of mice per cohort for this analysis were WT (n = 25), *53BP1*$^{-/-}$ (n = 30), *Brca1*$^{\Delta11/\Delta11}$*53BP1*$^{-/-}$ (n = 35), and *Brca1*$^{\Delta11/\Delta11}$ *p53*$^{+/-}$ (n = 21).

exogenous and perhaps stronger DNA-damaging stresses, the recruitment of additional factors somehow lessens the ultimate requirement for 53BP1 expression.

There is a growing realization that the accumulation of senescent and apoptotic cells might contribute to organismal aging, as well as serving as a barrier to tumor formation (Bartkova et al., 2005, 2006; Braig et al., 2005; Chen et al., 2005; Collado et al., 2005; Di Micco et al., 2006; Gorgoulis et al., 2005; Michaloglou et al., 2005). One of the interesting observations from the current study is the extended life span and near-wild-type appearance of *Brca1*$^{\Delta11/\Delta11}$*53BP1*$^{-/-}$ mice. The relative absence of various progeriod phenotypes (e.g., kyphosis, reduced skin thickness, osteoporosis, etc.) as well as the extended overall life span suggest that blocking cellular senescence and cell death mitigates the accelerated aging phenotype seen in this model of DNA damage. Perhaps more surprising are the observations that *Brca1*$^{\Delta11/\Delta11}$*53BP1*$^{-/-}$ mice exhibit genomic instability, yet still do not manifest a marked increase in tumor formation over the first 20 months of life. In previous examples where the *Brca1*$^{\Delta11/\Delta11}$ mice have been rescued from embryonic lethality, there was an extraordinarily high rate of subsequent malignancies. These high rates of tumor incidence include a near 100% incidence in *Brca1*$^{\Delta11/\Delta11}$*p53*$^{-/-}$ mice by 3 months of age (Bachelier et al., 2003; Brodie et al., 2001; Xu et al., 2001) and a greater than 70% incidence of breast cancer in female *Brca1*$^{\Delta11/\Delta11}$*Chk2*$^{-/-}$ mice by 16 months of age (Cao et al., 2006). One potential explanation for the relatively low levels of tumor formation in the *Brca1*$^{\Delta11/\Delta11}$*53BP1*$^{-/-}$ mice compared to previous results is that *Brca1*$^{\Delta11/\Delta11}$*53BP1*$^{-/-}$ cells appear to maintain an intact senescent and apoptotic response to various other stresses. In contrast, following exposure to a wide range of DNA-damaging stresses, mice deficient in either *Chk2* or *p53* are known to have a generalized and widespread impairment in their apoptotic and/or senescent response.

Recent evidence has suggested that there may some degree of commonality in the mechanisms underlying cancer and aging (DePinho, 2000; Finkel et al., 2007; Serrano and Blasco, 2007). As we have discussed, the accumulation of senescent cells may be beneficial in blocking tumorgenesis, yet harmful by contributing to organismal aging. As such, our current results provide a potentially instructive example of a model of DNA damage and genomic instability where it would appear that one can selectively ameliorate age-dependent pathologies without significantly increasing cancer rates. Further refinement of our understanding of the molecular pathways leading from DNA damage to cell death and senescence may ultimately allow for new strategies that directly combat age-related phenotypes without substantially altering the predisposition for cancer.

EXPERIMENTAL PROCEDURES

Mice and MEF Cells

53BP1$^{+/-}$ (Ward et al., 2003), *H2AX*$^{+/-}$ (Celeste et al., 2002), *Chk2*$^{+/-}$ (Takai et al., 2002), *Atm*$^{+/-}$ (Barlow et al., 1996), and *p53*$^{+/-}$ (Donehower et al., 1992) mice were analyzed alone or, where indicated, crossed with *Brca1*$^{+/\Delta11}$ mice (Xu et al., 2001) to generate double-mutant mice. MEF cells were derived from E14.5 embryos using standard methods and subsequently cultured in DMEM supplemented with 15% FBS.

Histological, Immunohistochemistry, and Protein Expression Analysis

For routine histology analysis, tissues were fixed in 10% formalin, blocked in paraffin, sectioned, stained with hematoxylin and eosin, and subsequently examined by light microscopy. Antibodies for 53BP1 (1:000, Novus Biologicals, LLC; Littleton, CO), γ-H2AX (1:000, Millipore Corporation; Billerica, MA), Rad51 (1:200, Santa Cruz Biotechnology, Inc.; Santa Cruz, CA), MDC1 (1:200, Abcam, Inc.; Cambridge, MA), H4K20me3, H4K20Me2, and H3K79 (all Abcam at 1:500) were employed for immunohistological analysis. Detection of the primary antibody was performed using the Histomouse TM Kit (Zymed Laboratories, Inc.; San Francisco) according to the manufacturer's instruction.

Western blot analysis was performed according to standard procedures using ECL detection (GE Healthcare; Buckinhamshire, UK). The following primary antibodies were used: p53 (BD Biosciences; San Jose, CA), p21 (Santa Cruz Biotechnology), ATM p-Ser1987 (BD Biosciences), Chk2 (Millipore), p53 p-Ser15 (Cell Signaling Technology, Inc.; Danvers, MA), and SMC1 (Novus Biologicals).

Senescence, Cell Death-Accelerated Aging, and Genomic Instability Assays

For SA-βgal analysis of MEFs, cells were washed with PBS (pH 7.2), fixed with 0.5% glutaraldehyde in PBS (pH 7.2), and processed as previously described (Dimri et al., 1995). For in vivo SA-βgal analysis, frozen sections were obtained and subsequently fixed in 1% formalin/PBS for 1 min prior to staining, while embryo senescence was determined as previously described (Cao et al., 2003). Where indicated, early-passage MEF cells were treated with 20 μM hydrogen peroxide or with 10 Gy γ irradiation, cultured for an additional 7 days, and then assessed for SA-βgal staining.

For assessment of cell death in vivo, we performed TUNEL assays on tissue sections on embryos at day E18 using the TUNEL kit (Millipore). Measurements of thymocyte cell death under basal conditions and following irradiation were performed using propidium iodide and a fluorogenic caspase-3 substrate, as previously described (Komoriya et al., 2000). Apoptosis of MEF cells treated with hydrogen peroxide (50 μM), doxorubicin (200 ng/ml), or 15 Gy γ irradiation was assessed 24 hr after treatment using propidium iodide (Sigma-Aldrich; St. Louis) staining and subsequent analysis for sub-G0/G1 events on a Becton Dickinson FACSCalibur.

Bone density was assessed by an X-ray dose of 15 kV for 100 s using a Faxitron X-ray apparatus. The analysis of genomic instability was performed on metaphases prepared from splenic B cells, enriched by CD43 MACS depletion (Miltenyi Biochnology; Bergisch Gladbach, Germany). Isolated B cells were cultured for 60 hr with LPS and IL-4. The metaphases were prepared by standard protocols (hypotonic lysis with fixation in 3:1 methanol:acetic acid) on colcemid-arrested cells as previously described (Callén et al., 2007).

SUPPLEMENTAL DATA

Supplemental Data include one table and seven figures and can be found online at http://www.cell.com/molecular-cell/supplemental/S1097-2765(09)00548-6.

ACKNOWLEDGMENTS

We are grateful to N. Motoyama for the generous gift of *Chk2*$^{-/-}$ mice. This work was supported by NIH Intramural funds and a grant from the Ellison Medical Foundation (T.F.).

Received: January 22, 2009
Revised: May 1, 2009
Accepted: June 17, 2009
Published: August 27, 2009

REFERENCES

Adams, M.M., and Carpenter, P.B. (2006). Tying the loose ends together in DNA double strand break repair with 53BP1. Cell Div. *1*, 19.

Bachelier, R., Xu, X., Wang, X., Li, W., Naramura, M., Gu, H., and Deng, C.X. (2003). Normal lymphocyte development and thymic lymphoma formation in Brca1 exon-11-deficient mice. Oncogene *22*, 528–537.

Barlow, C., Hirotsune, S., Paylor, R., Liyanage, M., Eckhaus, M., Collins, F., Shiloh, Y., Crawley, J.N., Ried, T., Tagle, D., and Wynshaw-Boris, A. (1996). Atm-deficient mice: a paradigm of ataxia telangiectasia. Cell *86*, 159–171.

Bartkova, J., Horejsí, Z., Koed, K., Krämer, A., Tort, F., Zieger, K., Guldberg, P., Sehested, M., Nesland, J.M., Lukas, C., et al. (2005). DNA damage response as a candidate anti-cancer barrier in early human tumorigenesis. Nature *434*, 864–870.

Bartkova, J., Rezaei, N., Liontos, M., Karakaidos, P., Kletsas, D., Issaeva, N., Vassiliou, L.V., Kolettas, E., Niforou, K., Zoumpourlis, V.C., et al. (2006). Oncogene-induced senescence is part of the tumorigenesis barrier imposed by DNA damage checkpoints. Nature *444*, 633–637.

Botuyan, M.V., Lee, J., Ward, I.M., Kim, J.E., Thompson, J.R., Chen, J., and Mer, G. (2006). Structural basis for the methylation state-specific recognition of histone H4-K20 by 53BP1 and Crb2 in DNA repair. Cell *127*, 1361–1373.

Braig, M., Lee, S., Loddenkemper, C., Rudolph, C., Peters, A.H., Schlegelberger, B., Stein, H., Dörken, B., Jenuwein, T., and Schmitt, C.A. (2005). Oncogene-induced senescence as an initial barrier in lymphoma development. Nature *436*, 660–665.

Brodie, S.G., Xu, X., Qiao, W., Li, W.M., Cao, L., and Deng, C.X. (2001). Multiple genetic changes are associated with mammary tumorigenesis in Brca1 conditional knockout mice. Oncogene *20*, 7514–7523.

Callén, E., Jankovic, M., Difilippantonio, S., Daniel, J.A., Chen, H.T., Celeste, A., Pellegrini, M., McBride, K., Wangsa, D., Bredemeyer, A.L., et al. (2007). ATM prevents the persistence and propagation of chromosome breaks in lymphocytes. Cell *130*, 63–75.

Cao, L., Li, W., Kim, S., Brodie, S.G., and Deng, C.X. (2003). Senescence, aging, and malignant transformation mediated by p53 in mice lacking the Brca1 full-length isoform. Genes Dev. *17*, 201–213.

Cao, L., Kim, S., Xiao, C., Wang, R.H., Coumoul, X., Wang, X., Li, W.M., Xu, X.L., De Soto, J.A., Takai, H., et al. (2006). ATM-Chk2-p53 activation prevents tumorigenesis at an expense of organ homeostasis upon Brca1 deficiency. EMBO J. *25*, 2167–2177.

Celeste, A., Petersen, S., Romanienko, P.J., Fernandez-Capetillo, O., Chen, H.T., Sedelnikova, O.A., Reina-San-Martin, B., Coppola, V., Meffre, E., Difilippantonio, M.J., et al. (2002). Genomic instability in mice lacking histone H2AX. Science *296*, 922–927.

Chen, J.H., Hales, C.N., and Ozanne, S.E. (2007). DNA damage, cellular senescence and organismal ageing: causal or correlative? Nucleic Acids Res. *35*, 7417–7428.

Chen, Z., Trotman, L.C., Shaffer, D., Lin, H.K., Dotan, Z.A., Niki, M., Koutcher, J.A., Scher, H.I., Ludwig, T., Gerald, W., et al. (2005). Crucial role of p53-dependent cellular senescence in suppression of Pten-deficient tumorigenesis. Nature *436*, 725–730.

Clarke, A.R., Purdie, C.A., Harrison, D.J., Morris, R.G., Bird, C.C., Hooper, M.L., and Wyllie, A.H. (1993). Thymocyte apoptosis induced by p53-dependent and independent pathways. Nature *362*, 849–852.

Collado, M., Gil, J., Efeyan, A., Guerra, C., Schuhmacher, A.J., Barradas, M., Benguria, A., Zaballos, A., Flores, J.M., Barbacid, M., et al. (2005). Tumour biology: senescence in premalignant tumours. Nature *436*, 642.

DePinho, R.A. (2000). The age of cancer. Nature *408*, 248–254.

Di Micco, R., Fumagalli, M., Cicalese, A., Piccinin, S., Gasparini, P., Luise, C., Schurra, C., Garre', M., Nuciforo, P.G., Bensimon, A., et al. (2006). Oncogene-induced senescence is a DNA damage response triggered by DNA hyper-replication. Nature *444*, 638–642.

Dimri, G.P., Lee, X., Basile, G., Acosta, M., Scott, G., Roskelley, C., Medrano, E.E., Linskens, M., Rubelj, I., Pereira-Smith, O., et al. (1995). A biomarker that identifies senescent human cells in culture and in aging skin in vivo. Proc. Natl. Acad. Sci. USA *92*, 9363–9367.

Donehower, L.A., Harvey, M., Slagle, B.L., McArthur, M.J., Montgomery, C.A., Jr., Butel, J.S., and Bradley, A. (1992). Mice deficient for p53 are developmentally normal but susceptible to spontaneous tumours. Nature *356*, 215–221.

Finkel, T., Serrano, M., and Blasco, M.A. (2007). The common biology of cancer and ageing. Nature *448*, 767–774.

Gorgoulis, V.G., Vassiliou, L.V., Karakaidos, P., Zacharatos, P., Kotsinas, A., Liloglou, T., Venere, M., Ditullio, R.A., Jr., Kastrinakis, N.G., Levy, B., et al. (2005). Activation of the DNA damage checkpoint and genomic instability in human precancerous lesions. Nature *434*, 907–913.

Hakem, R., de la Pompa, J.L., Elia, A., Potter, J., and Mak, T.W. (1997). Partial rescue of Brca1 (5-6) early embryonic lethality by p53 or p21 null mutation. Nat. Genet. *16*, 298–302.

Hirao, A., Kong, Y.Y., Matsuoka, S., Wakeham, A., Ruland, J., Yoshida, H., Liu, D., Elledge, S.J., and Mak, T.W. (2000). DNA damage-induced activation of p53 by the checkpoint kinase Chk2. Science *287*, 1824–1827.

Huyen, Y., Zgheib, O., Ditullio, R.A., Jr., Gorgoulis, V.G., Zacharatos, P., Petty, T.J., Sheston, E.A., Mellert, H.S., Stavridi, E.S., and Halazonetis, T.D. (2004). Methylated lysine 79 of histone H3 targets 53BP1 to DNA double-strand breaks. Nature *432*, 406–411.

Komoriya, A., Packard, B.Z., Brown, M.J., Wu, M.L., and Henkart, P.A. (2000). Assessment of caspase activities in intact apoptotic thymocytes using cell-permeable fluorogenic caspase substrates. J. Exp. Med. *191*, 1819–1828.

Lombard, D.B., Chua, K.F., Mostoslavsky, R., Franco, S., Gostissa, M., and Alt, F.W. (2005). DNA repair, genome stability, and aging. Cell *120*, 497–512.

Lowe, S.W., Schmitt, E.M., Smith, S.W., Osborne, B.A., and Jacks, T. (1993). p53 is required for radiation-induced apoptosis in mouse thymocytes. Nature *362*, 847–849.

Ludwig, T., Chapman, D.L., Papaioannou, V.E., and Efstratiadis, A. (1997). Targeted mutations of breast cancer susceptibility gene homologs in mice: lethal phenotypes of Brca1, Brca2, Brca1/Brca2, Brca1/p53, and Brca2/p53 nullizygous embryos. Genes Dev. *11*, 1226–1241.

Michaloglou, C., Vredeveld, L.C., Soengas, M.S., Denoyelle, C., Kuilman, T., van der Horst, C.M., Majoor, D.M., Shay, J.W., Mooi, W.J., and Peeper, D.S. (2005). BRAFE600-associated senescence-like cell cycle arrest of human naevi. Nature *436*, 720–724.

Parrinello, S., Samper, E., Krtolica, A., Goldstein, J., Melov, S., and Campisi, J. (2003). Oxygen sensitivity severely limits the replicative lifespan of murine fibroblasts. Nat. Cell Biol. *5*, 741–747.

Riley, T., Sontag, E., Chen, P., and Levine, A. (2008). Transcriptional control of human p53-regulated genes. Nat. Rev. Mol. Cell Biol. *9*, 402–412.

Rodier, F., Campisi, J., and Bhaumik, D. (2007). Two faces of p53: aging and tumor suppression. Nucleic Acids Res. *35*, 7475–7484.

Serrano, M., and Blasco, M.A. (2007). Cancer and ageing: convergent and divergent mechanisms. Nat. Rev. Mol. Cell Biol. *8*, 715–722.

Takai, H., Naka, K., Okada, Y., Watanabe, M., Harada, N., Saito, S., Anderson, C.W., Appella, E., Nakanishi, M., Suzuki, H., et al. (2002). Chk2-deficient mice exhibit radioresistance and defective p53-mediated transcription. EMBO J. *21*, 5195–5205.

van Attikum, H., and Gasser, S.M. (2009). Crosstalk between histone modifications during the DNA damage response. Trends Cell Biol. *19*, 207–217.

Ward, I.M., Minn, K., van Deursen, J., and Chen, J. (2003). p53 Binding protein 53BP1 is required for DNA damage responses and tumor suppression in mice. Mol. Cell. Biol. *23*, 2556–2563.

Xu, X., Qiao, W., Linke, S.P., Cao, L., Li, W.M., Furth, P.A., Harris, C.C., and Deng, C.X. (2001). Genetic interactions between tumor suppressors Brca1 and p53 in apoptosis, cell cycle and tumorigenesis. Nat. Genet. *28*, 266–271.